Contribution from the Department of Chemistry, Rutgers, The State University of New Jersey, New Brunswick, New Jersey 08903, and AT&T Bell Laboratories, Murray Hill, New Jersey 07974

# Lithium Insertion Compounds of the High- and Low-Temperature Polymorphs of $LiFeSnO_4$

M. GREENBLATT,*† E. WANG,† H. ECKERT,† N. KIMURA,† R. H. HERBER,*† and J. V. WASZCZAK‡

*Received August 16, 1984*

The high-temperature (HT) and low-temperature (LT) polymorphs of $LiFeSnO_4$ with ramsdellite-related structures undergo lithium insertion reactions with *n*-BuLi at ambient temperature to stoichiometries $Li_2FeSnO_4$ (HT) and $Li_{1.8}FeSnO_4$ (LT). We report crystal–chemical data for the lithium insertion compounds and the behavior of the host compounds mixed with graphite as the positive electrodes in small lithium secondary test cells. $^{57}Fe$ Mössbauer studies confirm the reduction of $Fe^{3+}$ to $Fe^{2+}$ in the lithiated compounds. $^{119}Sn$ Mössbauer results show subtle differences of Sn–O bonding and distortion of the $SnO_6$ polyhedra in the two polymorphs. Magnetic susceptibility vs. temperature data show strong exchange interactions in both polymorphs and their lithiated analogues.

## Introduction

Compounds that can reversibly incorporate lithium ions into their crystal structures are of interest for application as cathode materials in secondary batteries. Lithium insertion reactions of $ReO_3$, $WO_3$, and various structurally related vanadium and niobium oxide shear structures have been reported.[1-5] These compounds have three-dimensional network structures of corner and/or edge-sharing metal–oxygen octahedra ($MO_6$) with large cubooctahedral cavities. The tunnellike vacancies are interconnected in three dimensions, allowing the fast and reversible diffusion of lithium ions.

Two polymorphous lithium stannoferrites, $LiFeSnO_4$, a high-temperature (HT) ramsdellite-type, and a low-temperature (LT) hexagonal close-packed structure are known.[6,7] X-ray and neutron powder diffraction structural refinement of each showed that orthorhombic $LiFeSnO_4$ (HT) is isostructural with ramsdellite $\gamma$-$MnO_2$, in which the tunnels are partially occupied by lithium ions. The projection of the structure of this compound along [1, 0, 0] is shown in Figure 1. The host lattice is built up of edge-sharing $SnO_6$ and $FeO_6$ octahedra, with a statistical distribution of metallic ions forming rectangular tunnels along the [1, 0, 0] direction.[6,7] In the tunnels, there are five possible sites: four tetrahedral ($T_1$, $T_2$, $T_3$, $T_4$) and one octahedral (Oc). In $LiFeSnO_4$ (HT), the lithium ions occupy the $T_1$ and $T_2$ tetrahedral sites, with a preferential occupancy of the $T_1$ sites ($\sim$76%). Taking into account the distances between two neighboring sites, four A cations per cell can be located in these tunnels, leading to the limiting formula $A_4B_4O_8$. $LiFeSnO_4$ (HT) can thus be considered as a partially occupied ramsdellite.

Hexagonal $LiFeSnO_4$ (LT) is structually very similar to the high-temperature phase. The main difference between the two structures is the distribution of metallic ions, which has been confirmed to be $(Li_{0.56}Fe_{0.44})_{T_1}(Li)_{T_2}(Sn)_{Oc_1}(SnLi_{0.44}Fe_{1.56})_{Oc_2}O_8$ by a neutron diffraction study.[7] Thus, tin is only located on the octahedral sites, while lithium and iron are distributed on both tetrahedral sites in the tunnel and octahedral sites of the framework structure. However, only $\sim$22% of the Li ions are located in octahedral sites and the same percentage of tetrahedral sites is occupied by Fe.

Partial occupation of the sites in the tunnel in both polymorphs of these stannoferrites suggested the possibility of lithium insertion. Moreover, previous results of solid-state reactions of $LiFeSnO_4$–$Li_2SnO_3$ indicated that the stability of the ramsdellite structure can be improved by introducing a greater amount of lithium into the ramsdellite tunnels.[7]

One of the reasons we have undertaken the study of lithium insertion in the $LiFeSnO_4$ phases was to provide a good model for lithium insertion in a reproducible, well-crystallized, ramsdellite material. In contrast, $\gamma$-$MnO_2$, which also has the ramsdellite structure and which is an important cathode material in secondary lithium batteries, has not been obtainable so far in good-quality crystalline form. We have carried out lithium insertion reactions on the two polymorphs of $LiFeSnO_4$ with *n*-butyllithium (*n*-BuLi) in hexane as well as by electrochemical means. We report here on the properties of these new lithium insertion compounds and the results of $^{57}Fe$ and $^{119}Sn$ Mössbauer spectroscopic studies.

## Experimental Section

$LiFeSnO_4$ (HT) and $LiFeSnO_4$ (LT) were prepared according to the procedure of Choisnet et al.[6] Chemical lithiation of the compounds was carried out by treatment with *n*-BuLi in hexane at $\sim$25 °C. The amount of lithium consumed in the reaction was determined by acid–base titration of the excess *n*-BuLi and by plasma emission spectroscopy of the lithiated products. Delithiation reactions were carried out on the lithium-inserted compounds with iodine in acetonitrile ($I_2/CH_3CN$). The amount of iodine reacted was determined by titration of the excess with standard thiosulfate solution.

The host and lithium-inserted phases were characterized by powder X-ray diffraction. Patterns were recorded in the range $10° \leq 2\theta \leq 80°$ at 1°/min, with Cu K$\alpha$ radiation. Observed peak positions for all samples were calibrated against an internal silicon standard. The X-ray diffraction patterns of the iodine-delithiated phases were also recorded and compared to those of the initial host compounds to check for irreversible structural changes due to lithium insertion. The thermal stability of the inserted phases was determined by differential scanning calorimetry. Samples were heated at 20°/min in sealed He-filled Al capsules and heated to $\sim$600 °C on a Du Pont 943 computer-controlled thermal analyzer system. Small electrochemical test cells[8] were fabricated with $LiFeSnO_4$ (HT) and $LiFeSnO_4$ (LT), respectively, mixed with 20 wt % graphite as cathode and 1 M $LiClO_4$/propylene carbonate (PC) as electrolyte.

The open-circuit potential for a particular value of $x$ was obtained by measuring the voltage of the cell immediately after the appropriate amount of current was allowed to pass through it. The potential of the cell was then measured in 24-h intervals (for several days if required) until a constant potential, indicative of the equilibrium potential values shown in Figures 2 and 3, was obtained.

The magnetic susceptibility was measured by using the Faraday method as described previously.[9] $^{57}Fe$ and $^{119}Sn$ Mössbauer experiments were carried out in transmission geometry, using Pd ($^{57}Co$) and $CaSnO_3$ ($^{119}Sn$) sources, respectively. All isomer shifts for the iron spectra are referred to the centroid of an absorption spectrum of NBS-SRM metallic iron (which was also used to calibrate the velocity scale), while those for tin spectra are referred to the absorption centroid of $CaSnO_3$, both at 295

†Rutgers, The State University of New Jersey.
‡AT&T Bell Laboratories.

(1) Whittingham, M. S. *Prog. Solid State Chem.* **1978**, *12*, 1.
(2) Murphy, D. W.; Christian, P. A. *Science (Washington, D.C.)* **1979**, *No. 205*, 651.
(3) Murphy, D. W.; Greenblatt, M.; Cava, R. J.; Zahurak, S. M. *Solid State Ionics* **1981**, *5*, 327.
(4) Cheng, K. H.; Whittingham, M. S. *Solid State Ionics* **1980**, *1*, 151.
(5) Cava, R. J.; Murphy, D. W.; Zahurak, S. M. *J. Electrochem. Soc.* **1983**, *130*, 2345.
(6) Choisnet, J.; Hervieu, M.; Raveau, B.; Tarte, P. *J. Solid State Chem.* **1981**, *40*, 344.
(7) Lacorre, P.; Hervieu, M.; Pannetier, J.; Choisnet, J.; Raveau, B. *J. Solid State Chem.* **1983**, *50*, 196.
(8) Murphy, D. W.; Carides, J. N.; DiSalvo, F. J.; Cros, C.; Waszczak, J. V. *Mat. Res. Bull.* **1977**, *12*, 825.
(9) DiSalvo, F. J.; Waszczak, J. V. *Phys. Rev.* **1981**, *B23*, 457.

0020-1669/85/1324-1661$01.50/0 

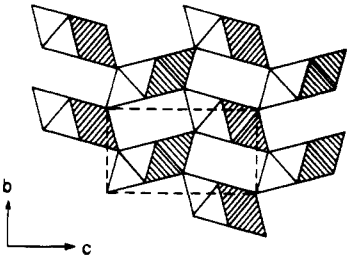


**Figure 1.** Ideal ramsdellite structure projected onto [1, 0, 0] plane.[7]

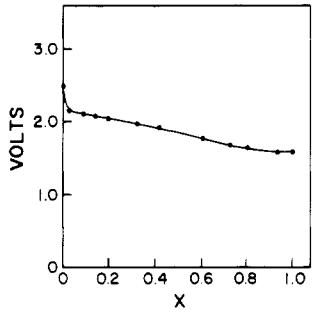


**Figure 2.** Open-circuit voltage vs. $x$ for Li|1 M $LiClO_4$,PC|$Li_{1+x}FeSnO_4$ (HT), graphite.

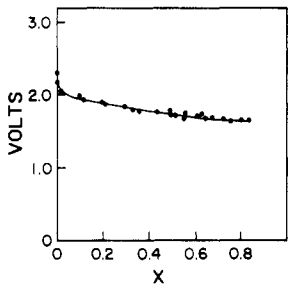


**Figure 3.** Open-circuit voltage vs. $x$ for Li|1 M $LiClO_4$,PC|$Li_{1+x}FeSnO_4$ (LT), graphite.

K. Samples of controlled thickness for $LiFeSnO_4$ (both the HT and LT form) were prepared by dispersing the absorber material in an inert carbohydrate matrix and compressing this into a weighable pellet that was then clamped into a thermally shielded variable-temperature cryostat as described previously.[10]

Mössbauer data reduction was effected using a matrix-inversion least-squares routine on the Rutgers NS 9000 computer. Line positions, widths, and intensities were allowed to vary as free parameters. The sample thickness was adjusted such that the line was unaffected by saturation broadening effects over the temperature range studied.

## Results and Discussion

**a. Physicochemical Properties.** On lithium insertion, the brown $LiFeSnO_4$ (HT) and dark brown $LiFeSnO_4$ (LT) changed to black within $\sim^1/_2$ h. Several days of lithiation by *n*-BuLi in hexane with mechanical stirring at room temperature resulted in $Li_2FeSnO_4$ (HT) and $Li_{1.8}FeSnO_4$ (LT) stoichiometries. This corresponds to the limits of the formula $A_4B_4O_8$ predicted for ramsdellite with maximum possible occupation of sites in the tunnels.[6] Electrochemical reactions carried out in Li/$LiClO_4$, PC/$LiFeSnO_4$ (HT), graphite and Li/$LiClO_4$, PC/$LiFeSnO_4$ (LT), graphite test cells yielded stoichiometries identical with those obtained by the *n*-BuLi reactions. Open-circuit voltages of representative cells as a function of lithium composition ($x$) are summarized graphically in Figures 2 and 3, respectively.

Powder X-ray diffraction patterns for both lithiated compounds are similar to those for the starting materials, but with significant changes in the unit cell parameters. The cell parameters, compared to the original unit cell dimensions, are presented in Table I. For both the HT and LT lithiated polymorphs the unit cell parameters increase linearly with successive lithiation; however, the increase is significantly larger along the $b$ and $c$ axes in $Li_2FeSnO_4$ (HT) and along $c$ in $Li_{1.8}FeSnO_4$ (LT) than along the $a$ unit cell dimension in each. This is consistent with their structural properties (Figure 1) in which the $b$ and $c$ directions correspond to the in-plane dimensions of the tunnel which must increase with increasing lithium content. On the other hand, there is more available space along the tunnels in the direction of the $a$ axis, in accordance with a much smaller increase in the $a$ parameter as observed in both lithiated compounds. It is probable that part of the observed unit cell dimension increase on lithiation is associated with the increase in the effective ionic radii in reducing $Fe^{3+}$ (high spin, hs) to $Fe^{2+}$ (hs). The great similarity of unit cell dimensions and X-ray powder pattern intensities of the lithiated and unlithiated polymorphs, respectively, suggests that there has not been extensive distortion of the host lattice on Li insertion. Delithiation of the fully lithiated phases by $I_2/CH_3CN$ restores the original color and the X-ray pattern of the host compounds. Furthermore, the shape of the EMF curves (Figures 2 and 3) also supports occurrence of reversible topotactic lithium insertion and suggests a continuous homogeneous single-phase region up to $Li_2FeSnO_4$ (HT) and $Li_{1.8}FeSnO_4$ (LT), respectively.

**Table I.** Crystallographic Unit Cell Parameters for Lithiated and Host Lithium Stannoferrites

| compd | $a_0$, Å | $b_0$, Å | $c_0$, Å | $V$, Å$^3$ |
|---|---|---|---|---|
| $LiFeSnO_4$ (HT)[a] | 3.066 | 5.066 | 9.874 | 153.4 |
| $Li_2FeSnO_4$ (HT)[b] | 3.080 | 5.130 | 9.993 | 157.9 |
| $LiFeSnO_4$ (LT)[a] | 6.012 | | 9.776 | |
| $Li_{1.8}FeSnO_4$ (LT)[b] | 6.030 | | 9.998 | |

[a] Unit cell data from ref 6. [b] Error in the unit cell parameters is ±0.004 Å.

The fully lithiated compounds were found by differential-scanning calorimetry to undergo changes, suggesting decomposition at approximately ~600 °C for $Li_2FeSnO_4$ (HT) and ~550 °C for $Li_{1.8}FeSnO_4$ (LT). The amorphous powder X-ray diffraction patterns of samples obtained after this heat treatment confirm these results.

Qualitative measurement of the electrical resistivity at room temperature on pressed powder pellets indicates that both HT and LT polymorphs are insulating ($R > 10^6\Omega$). The lithiated compounds show a significant increase in the conductivity ($R \sim 10^3\Omega$) under identical experimental conditions, and the LT phase has a conductivity approximately 1 order of magnitude larger than the HT analogue. In the fully lithiated HT form the expected oxidation states of the cations are $Li_2Fe^{2+}Sn^{4+}O_4$. The significant increase in the conductivity of $Li_2FeSnO_4$ relative to the unlithiated host is most likely due to the presence of a small concentration of $Fe^{3+}$ ions (supported by the Mössbauer data as discussed below) that facilitate charge hopping. In the LT form the fully lithiated phase has a stoichiometry of $Li_{1.8}FeSnO_4$ (LT) whether obtained by the *n*-BuLi reaction or by electrochemical means. Because ~22% of the tetrahedral tunnel sites are already occupied by Fe in the host compound, lithium insertion can only occur to the observed limit of 0.8 per formula unit. This leads to the presence of substantial amounts of mixed-valent iron ($Li_{1.8}Fe_{0.8}^{2+}Fe_{0.2}^{3+}Sn O_4$, which is also confirmed by the Mössbauer results), which may explain why the electrical conductivity of this compound is substantially higher than that of $Li_2FeSnO_4$ (HT) in which essentially all of the $Fe^{3+}$ is reduced.

**b. Mössbauer Results.** The $^{57}Fe$ Mössbauer parameters of the two host matrices are summarized in Table II and are typical of high-spin iron(III) oxide compounds. A comparison of the spectra pertaining to the HT and LT phases reveals significant differences, indicating substantially higher bond ionicity and a more symmetric local iron coordination in the high-temperature form. The LT phase shows some excess line broadening ($\Gamma \approx 0.50$ mm/s, independent of temperature) that possibly reflects the distribution of iron between octahedral and tetrahedral sites, as discussed above.

Figures 4 and 5 show the change of the Mössbauer spectra (at 78 K) upon successive electrochemical lithiation. For both the

(10) See, for example: Herber, R. H.; Shanzer, A; Libman, J. *Organometallics* **1984**, *3*, 586 and references therein.

**Table II.** $^{57}$Fe Mössbauer Effect Data for the Compounds Discussed in the Text

| compd | $LiFeSnO_4$ (LT) | $LiFeSnO_4$ (HT) | $Li_{1.8}FeSnO_4$ (LT) | $Li_2FeSnO_4$ (HT) |
|---|---|---|---|---|
| IS(78 K),[a,c] mm $s^{-1}$ | 0.443 | 0.476 | 1.13[g] | 1.20[g] |
| IS(300 K), mm $s^{-1}$ | 0.325 | 0.365 | 0.88[h] | 1.07[h] |
| QS(78 K),[b,c] mm $s^{-1}$ | 0.758 | 0.450 | 2.39[g] | 2.73[g] |
| QS(300 K), mm $s^{-1}$ | 0.756 | 0.433 | 1.57[h] | 2.08[h] |
| $10^4$(dIS/d$T$),[d] mm $s^{-1}$ $K^{-1}$ | 5.26 (0.996) | 5.01 (0.997) | *j* | *j* |
| $10^4$[d[ln ($A(T)/A(78)$)]/d$T$],[e] $K^{-1}$ | 7.86 (0.996) | 6.10 (0.991) | *j* | *j* |
| $M_{eff}$,[i] g $mol^{-1}$ | 79.2 | 83.2 | *j* | *j* |
| $\Theta'_M$,[f] K | 353 | 392 | *j* | *j* |

[a] Isomer shift with respect to metallic iron at 295 ± 2 K. [b] Quadrupole splitting. [c] Estimated errors: ±0.010 mm $s^{-1}$ for HT, ±0.005 mm $s^{-1}$ for LT forms. [d] Temperature dependence of the isomer shift (linear correlation coefficient). [e] Temperature dependence of the recoil-free fraction (linear correlation coefficient). [f] Estimated error: ±5 K, calculated from eq 17 of ref 15. [g] Iron(II) site only; estimated error ±0.020 mm $s^{-1}$. [h] Spectra influenced by valence averaging; estimated error ±0.040 mm $s^{-1}$. [i] Calculated from eq 16′ of ref 15. [j] Not determined.

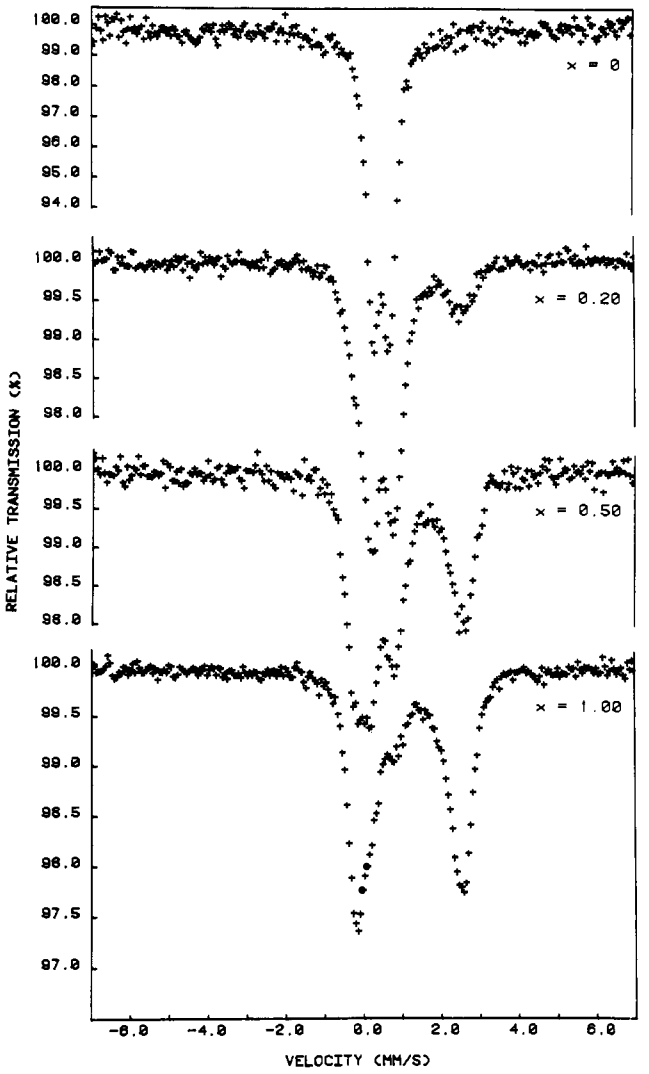


**Figure 4.** $^{57}$Fe Mössbauer spectra at 78 K of $Li_{1+x}FeSnO_4$ (HT) as a function of $x$.

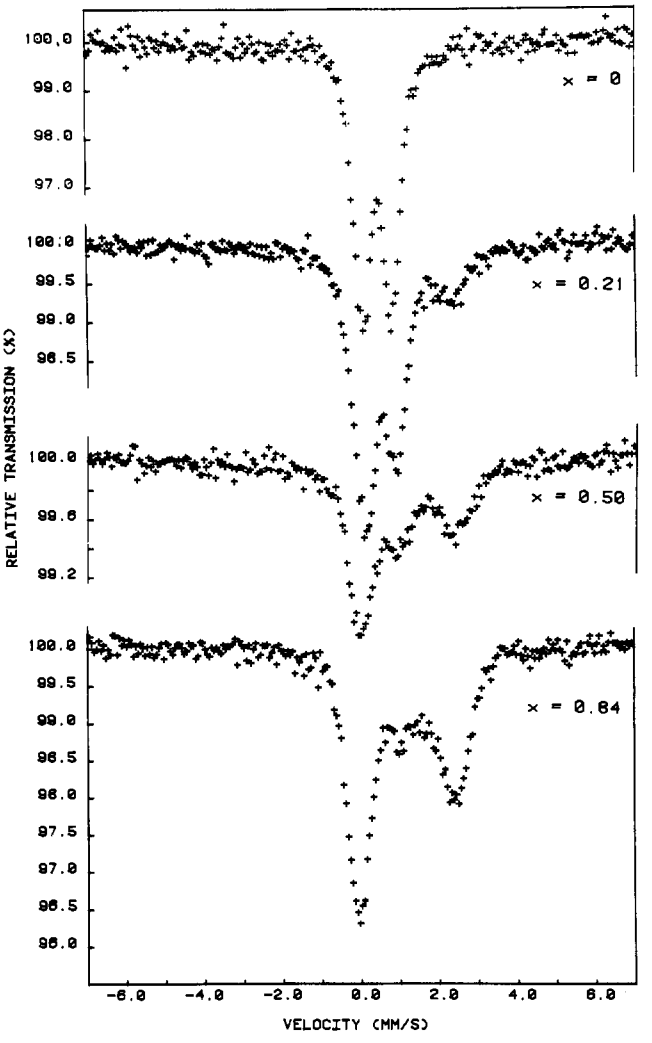


**Figure 5.** $^{57}$Fe Mössbauer spectra at 78 K of $Li_{1+x}FeSnO_4$ (LT) as a function of $x$.

HT and LT materials, results are identical for the charging and the discharging process, reflecting excellent mechanistic reversibility of the present electrode systems. This contrasts to the results of a previous Mössbauer study of the $LiKFeS_2$ cathode material, for which a significantly more complicated behavior was found.[11] For the present systems, the Mössbauer spectra (cf. Figures 4 and 5) clearly reveal that lithium insertion proceeds via the reduction of $Fe^{3+}$. At 78 K two superimposed quadrupole doublets are observed, the hyperfine parameters of which are consistent with $Fe^{3+}$ (hs) and $Fe^{2+}$ (hs). A more detailed analysis of the spectra is rendered somewhat ambiguous, since the lines are relatively broad ($\Gamma \sim 0.5$ mm/s), probably reflecting electric field gradient distribution effects. Notwithstanding this limitation, the total amount of $Fe^{2+}$ as determined by doubling the fractional area of the high-velocity peak at ~2.3 mm/s is in very good agreement with the nominal amount of charge transferred during the electrochemical preparation. Only at large values of $x$ ($x \geq 0.9$) is some deviation from linearity noticeable, arising from the presence of some residual $Fe^{3+}$ in $Li_{2.0}FeSnO_4$. Assuming equal recoil-free fractions for the $Fe^{3+}$ and $Fe^{2+}$ sites in this compound at 78 K, the fraction of $Fe^{3+}$ can be estimated from the respective areas under the resonance curves and corresponds to ~21% for $x = 1.0$. This observation is probably due to the fact that the electrochemical lithiation is accompanied by a minor charge-consuming side-reaction that leads to a slight overestimation of the lithium content as determined from the amount of the transferred charge. The voltage/composition plot of the HT phase (Figure 2) plateaus at $x > 0.9$, suggesting, as the Mössbauer data

(11) Jacobson, A. J.; McCandlish, L. E. *J. Solid State Chem.* **1979**, *19*, 355.

**Table III.** $^{119}$Sn Mössbauer Effect Data for the Compounds Discussed in the Text

| compd | $LiFeSnO_4$ (LT) | $LiFeSnO_4$ (HT) | $Li_{1.8}FeSnO_4$ (LT) | $Li_2FeSnO_4$ (HT) |
|---|---|---|---|---|
| IS(78 K),[a] mm $s^{-1}$ | 0.130 ± 0.020 | 0.129 ± 0.020 | 0.199 ± 0.015 | 0.196 ± 0.013 |
| IS(300 K),[a] mm $s^{-1}$ | 0.058 | 0.062 | 0.128 | 0.131 |
| QS,[b] mm $s^{-1}$ | 0.693 ± 0.020 | 0.446 ± 0.006 | 0.588 ± 0.009 | 0.502 ± 0.005 |
| $10^4(dIS/dT)$,[c] mm $s^{-1}$ $K^{-1}$ | 2.40 | 2.25 | 2.35 | 2.51 |
| $10^3[d[\ln (A(T)/A(78))]/dT]$,[c] $K^{-1}$ | 1.292 | 1.400 | 1.257 | 1.362 |
| $M_{eff}$,[d] g $mol^{-1}$ | 173 | 185 | 177 | 165 |
| $\Theta'_M$,[e] K | 308 | 286 | 309 | 307 |
| Γ(295 K),[f] mm $s^{-1}$ | 0.99 ± 0.07 | 0.84 ± 0.04 | 1.020 ± 0.042 | 0.957 ± 0.30 |

[a] Isomer shift with respect to $BaSnO_3$ at 295 ± 2 K. The isomer shifts of $BaSnO_3$, $CaSnO_3$, and $SnO_2$ are within the quoted errors. [b] Quadrupole splitting, assumed to be temperature independent within the quoted experimental errors. [c] For definition, see footnotes of Table II. [d] Calculated from eq 16′ of ref 15. [e] ±5 K; calculated from eq 17 of ref 15. [f] Full width at half-maximum.

do, that the end point for $Li_2FeSnO_4$ may be overestimated. Mössbauer spectra of the lithiated compounds containing the maximum amount of lithium prepared via the *n*-butyllithium reaction show good agreement with those obtained by the electrochemical technique.

Above 78 K, the spectra of all lithiated samples show continuous line broadening, decreasing quadrupole splitting, and a successive disappearance of the respective minority valency site as the temperature is increased. As has been demonstrated recently for FeOCl–Lewis base intercalates, these phenomena may reflect a charge-hopping process occurring on the time scale of the $^{57}$Fe Mössbauer effect.[12] It has also been noted that relaxation theory can provide a quantitative description of this valence-averaging process and that dynamical information can be extracted from temperature-dependent Mössbauer spectra.[13] For the present systems such studies are currently in progress and will be the subject of a future paper.[14]

At low temperatures (<30 K) the $^{57}$Fe Mössbauer spectra of each host and its lithiated analogue show increasing broadening of the absorption lines with decreasing temperature, which finally (<20 K) split into a six-line hyperfine pattern indicative of magnetic ordering. The shape and general quality of the spectra are typical of disordered magnetic interactions, in agreement with the magnetic susceptibility results discussed below.

The $^{119}$Sn Mössbauer parameters of the two host matrices, as well as of the lithium insertion compounds of each, are summarized in Table III. Precision data for $BaSnO_3$ and $CaSnO_3$, in which the local chemical environments around the tin atom are similar to those of the subject compounds, have recently been reported.[15] The isomer shifts observed in all of the compounds are characteristic of tin in the 4+ oxidation state, and the lithiation of $LiFeSnO_4$ does not result in reduction of the Sn to a lower valence state. The isomer shifts observed for both the LT and HT form of $LiFeSnO_4$ are identical and are significantly more positive than those determined for $CaSnO_3$ and $BaSnO_3$ in which the tin atoms occupy crystallograpically identical sites of cubic symmetry. The increase in the 5s electron density of the tin nucleus in the $LiFeSnO_4$ polymorphs, as compared to the perovskite structures $CaSnO_3$ and $BaSnO_3$, presumably arises from the distortion of the nearest-neighbor oxygen environment from ideal $O_h$ symmetry. On lithium insertion, the isomer shift increases still further and is again identical (within experimental error) for the LT and HT matrices.

The temperature dependence of the isomer shift[15] yields a value for the effective vibrating mass of the Mössbauer probe atom in these solids, and these data are included in Table III. The calculated values, 178 ± 8 amu, are identical for all of the octahedrally oxygen-coordinated tin atoms and reflect the significant covalency of the Sn–O bond. No systematic changes in this parameter on lithiation of the $LiFeSnO_4$ hosts can be discerned from the available data.

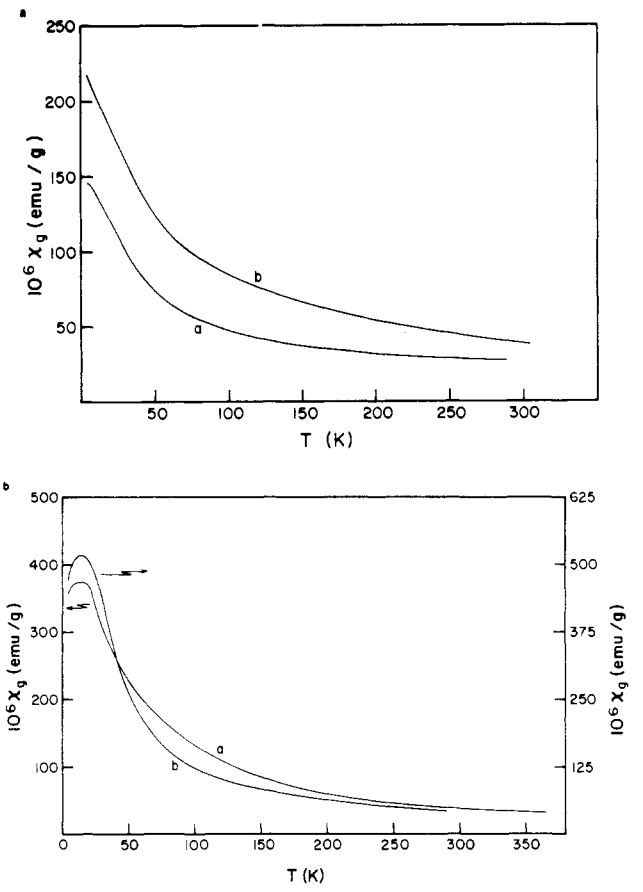


**Figure 6.** Temperature variation of the magnetic susceptibility: (a) (a) $LiFeSnO_4$ (HT) and (b) $Li_2FeSnO_4$ (HT); (b) (a) $LiFeSnO_4$ (LT) and (b) $Li_{1.8}FeSnO_4$ (LT).

Turning next to the quadrupole hyperfine interaction parameter extracted from the $^{119}$Sn Mössbauer data (Table III), it is seen that the distortion from ideal octahedral symmetry around the Sn atom gives rise to a detectable quadrupole splitting, which is larger in the LT form of $LiFeSnO_4$ than in the HT form, and that this difference is also observed in the two respective lithium-inserted matrices, although the absolute values are somewhat smaller. It is interesting to note that in the lithiated compounds, in which almost all of the iron atoms (which are chemically bonded to the $SnO_6$ octahedra through Fe–O–Sn linkages) are reduced from 3+ to 2+, the electronic charge distribution around the Sn atom becomes slightly more spherically symmetric (as compared to the host $LiFeSnO_4$ lattice), in contrast to a priori expectations.

Two further points relating to the variable-temperature $^{119}$Sn data are worth mentioning in the context of the comparison of the host matrices and their lithiated analogues. The Mössbauer lattice temperatures, $\Theta'_M$, calculated from the temperature dependence of the area under the resonance curve and the temperature dependence of the isomer shift,[15] are essentially identical for the four absorbers, as summarized in Table III, are comparable to that calculated for $CaSnO_3$, and are significantly higher than

(12) Eckert, H.; Herber, R. H. *J. Chem. Phys.* **1984**, *80*, 4526.
(13) Herber, R. H.; Eckert, H. *Phys. Rev.* **1985**, *B31*, 34.
(14) Eckert, H.; Wang, E.; Kimura, N.; Greenblatt, M.; Herber, R. H., to be submitted for publication.
(15) Herber, R. H. In "Chemical Mössbauer Spectroscopy"; Herber, R. H., Ed.; Plenum Press: New York, 1984.

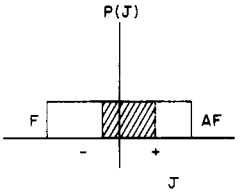


**Figure 7.** Ferromagnetic and antiferromagnetic exchange interaction constant $J$ vs. $P(J)$, the probability of a particular $J$.

the corresponding value for $BaSnO_3$. It is clear from these results that the lattice dynamical properties of the host materials probed by the $^{119}Sn$ Mössbauer resonance do not change significantly on lithium insertion and are identical (within experimental error) for the LT and HT forms of $LiFeSnO_4$, in contrast to the results extracted from the $^{57}Fe$ variable-temperature Mössbauer data for these two matrices.

**c. Magnetic Properties.** The magnetic susceptibility, $\chi$, of the HT phase measured from 300 to 4.2 K is shown in Figure 6a. It cannot be fit to a Curie–Weiss law in any range of the temperatures measured, with realistic values of the magnetic parameters. The exchange energies are very large, comparable to the temperatures in the range of measurement. Figure 7 shows a general plot of $J$, the magnetic exchange interaction constant, vs. $P(J)$, the probability of a particular $J$ for a system of magnetically interacting ions that might serve as a model for the observed magnetic properties. The behavior of the present compounds indicates that both ferromagnetic and antiferromagnetic interactions are present in a lattice of randomly distributed magnetic ions (as for example represented by the shaded region in Figure 7), resulting in an average net magnetic exchange effect. The susceptibility of the lithiated HT compound shown in Figure 6a gives a poor fit in the 100–300 K temperature range, with $\Theta \sim 100$ K, indicating a net antiferromagnetic interaction with fairly high exchange energies. The room-temperature susceptibilities $\chi_g$ are $26 \times 10^{-6}$ and $38 \times 10^{-6}$ emu/g for $LiFeSnO_4$ (HT) and $Li_2FeSnO_4$ (HT), respectively, indicating weaker exchange interactions in the lithiated phase. Assuming that the nature of the interactions remains the same, this result is in accordance with the lower magnetic moment expected for $Fe^{2+}$ ions ($S = 2$; vs. $Fe^{3+}$, $S = 2.5$). In addition it is possible that the increased density of $Li^+$ ions in the tunnels polarizes the oxygen orbitals, reducing their participation in the $Fe^{2+}$–O–$Fe^{2+}$ superexchange interactions.

The $\chi$ vs. $T$ of the LT phase of $LiFeSnO_4$ (Figure 6b) can be fit approximately to a Curie–Weiss law in the temperature range 100–400 K, with $\Theta \sim -26$ K. $\mu_{eff} \simeq 4.5\ \mu_B$ is significantly lower than 5.9 $\mu_B$ expected for high-spin octahedral $Fe^{3+}$; this might indicate a net antiferromagnetic interaction at room temperature. However, the ferromagnetic value of $\Theta$ at high temperature and the saturation of the susceptibility at low temperature suggest a disordered distribution of strong exchange interactions, also evidenced by a range of both positive and negative $\Theta$ values that can lead to spin glass behavior at low temperatures. Below the low-temperature transition at $\sim$20 K the susceptibility exhibits time dependence characteristic of a spin glass state.[16] The lithiated LT phase (Figure 6b) shows a low-temperature transition to a spin glass state similar to the unlithiated LT form. In the temperature range 100–400 K a rather poor fit to a Curie–Weiss law with $\Theta \sim 0$ K is obtained. The latter value indicates that the magnetic interactions have changed as compared to the unlithiated phase. Ferromagnetic pathways are not as dominant, because the oxidation state of iron has changed. There are $Fe^{3+}$–$Fe^{3+}$, $Fe^{2+}$–$Fe^{2+}$, and $Fe^{2+}$–$Fe^{3+}$ interactions possible. $\mu_{eff} \sim 5.0\ \mu_B$ is in good agreement with the calculated value of the effective magnetic moment for $Fe^{2+}$, which also tends to confirm that the exchange interactions are attenuated in the lithiated compound.

## Conclusion

The high- and low-temperature polymorphs of $LiFeSnO_4$ with $\gamma$-$MnO_2$ ramsdellite-type structures undergo reversible topotactic lithium insertion reactions with *n*-BuLi or by electrochemical means. Single-phase regions extending to the compositions $Li_2FeSnO_4$ (HT) and $Li_{1.8}FeSnO_4$ (LT) are observed. $^{57}Fe$ and $^{119}Sn$ Mössbauer spectra confirm that, upon lithiation of the host compounds, iron is reduced from high-spin $Fe^{3+}$ to high-spin $Fe^{2+}$ and that the oxidation state of tin remains 4+. In the LT compound $\sim$22% of the iron atoms are located in the tunnels of the ramsdellite lattice (sites where the Li atoms are located), and lithiation yields $Li_{1.8}Fe_{0.8}^{2+}Fe_{0.2}^{3+}SnO_4$ as confirmed qualitatively by the Mössbauer results. The electric conductivity of this phase is significantly larger than the conductivity of the host compounds or that of $Li_2Fe^{2+}SnO_4$ (HT), and evidence of dynamical charge hopping is observed. $Li_2FeSnO_4$ (HT), in addition to the majority $Fe^{2+}$ ions, also contains a small concentrations of $Fe^{3+}$ ions as indicated by the Mössbauer data and its increased electrical conductivity compared to the HT parent compound. The magnetic susceptibility of the HT host and its lithiated analogue cannot be fit to a Curie–Weiss law because of a random distribution of strong ferro- and antiferromagnetic interactions present. The susceptibility results of the LT phases show similarly strong magnetic exchange interactions and a transition to a spin glass state at $\sim$20 K.

**Acknowledgment.** The authors thank Dr. F. J. DiSalvo of Bell Laboratories for his substantial contributions to the interpretation of the magnetic susceptibility data. This work was supported in part by the Office of Naval Research (M.G.) and by the National Science Foundation-Solid State Chemistry, Grant DMR-81-02940 (to R.H.H.), as well as by a grant from the Center for Computer and Information Services, Rutgers University. This support is herewith gratefully acknowledged.

(16) Ford, P. J. *Contemp. Phys.* **1982**, *23*, 141.